Lithuanian Journal of Physics
Vol. 63, No. 3, pp. 140–147 (2023)
ISSN 1648-8504 eISSN 2424-3647
DOI: https://doi.org/10.3952/physics.2023.63.3.4

CHIRPED LG MODES INTERFERENCE FORMED CHIRAL BEAMS

G. Kontenis [a], D. Gailevičius [a], V. Jukna [a], and K. Staliūnas [a, b, c]

[a] *Laser Research Center, Vilnius University, Saulėtekio 10, 10223 Vilnius, Lithuania*
[b] *ICREA, Passeig Lluís Companys 23, 08010 Barcelona, Spain*
[c] *Dep. de Fisica, UPC, Rambla Sant Nebridi 22, 08222 Terrassa, Spain*
Email: gabrielius.kontenis@ff.vu.lt

Received 24 September 2023; accepted 25 September 2023

Non-Gaussian spatial intensity distribution beams used in laser micro- and nano-machining find many applications. For instance, Bessel beams, having a small diameter and a very long focal zone, allow the fabrication of high aspect ratio modifications in transparent materials. Higher-order Laguerre–Gauss modes are used in particle manipulation and even for multiplexing in optical communication. The temporal intensity distribution of a pulse is mostly overlooked or fixed to Gaussian shape distribution. However, pulse-shaped beams could improve the same fields of particle manipulation as optical traps, or the laser manufacturing. In this paper, we demonstrate a method of constructing a helical spatiotemporal intensity distribution beam the rotation of which in time can be varied. We demonstrate the analytical and numerical results and show an experimental realization of such a structure.

Keywords: chirped pulses, interference, orbital angular momentum

PACS: 42.65.Re, 42.25.Hz, 42.50.Tx

1. Introduction

Femtosecond (fs) lasers are becoming a preferred tool in laser processing and other areas [1–3]. Temporal structuring of pulses (i.e. compression to femtosecond range and tuning of repetition rate) provides control over the thermal aspect of processing [4, 5] and gives rise to cold ablation. In doing so, thermal effects are reduced, and more precise micromachining could be achieved, especially on thin materials that bend from the accumulated heat. One of the methods to achieve this is the use of burst pulses which is a trending way to achieve higher ablation efficiencies [6]. By having the sample ablated by a rotating intensity profile, there could be gaps in intensity enough to allow heat to flow out of the ablation region and reduce heat accumulation. A dynamic intensity pattern in the picosecond timeframe corresponding to the relaxation time of phonons could help further reduce the heat-affected zone (HAZ) around the machining area. One of the areas that saw substantial innovations in recent years is the use of spatially structured light [7–9]. The usage of advanced spatial light shaping techniques can lead to greatly increased fabrication efficiency [10–12], better processing quality [13–15] or both [16].

The vortex laser beams that have an orbital angular momentum provide a new degree of freedom for light manipulation and are widely applied in ablation [17], microscale matter manipulation, microscopy [18], and optical communications [19]. Nowadays, with the development of high-peak-power [20, 21], intense vortex laser pulses get attention for the interaction mechanisms with matter in strong-field laser physics.

A spatially spiralling beam has been shown in acoustics [22] and optics [23] by coaxially causing interference of two higher-order Bessel beams. In the acoustic case, the beam was generated by the use of axisymmetric spiral gratings [24–26]. While in the optical case, the beams were generated with a single element – a liquid crystal spatial light modulator (SLM). However, the resultant rotation can only be reached in the order of Hz by phase shifting one of the beams with different holograms. A different approach is necessary to increase the rotation speed relevant to manufacturing. Another way to increase the rotation speed is by using electro-optical or acoustic-optical elements to give rotation speeds in the order of GHz [27].

A recent alternative has been developed to work in the temporal domain, wherein two coherent chirped beams interfere to produce a rotating pattern in time [28, 29]. Such beams were termed 'vortex–pulse pairs'. These works are impressive, but they lack two things. First, focusing was not used as in Ref. [23] to produce a spatially winding structure – 'the optical drill'. Second, it appears that only an *EVEN* number of topological charges has been demonstrated: $\Delta l = 2, 4, 6$. However, there is no limitation on producing odd numbers of topological charges. In this work, we provided a replication study focusing on the *ODD* topological charge difference, wherein we have no mirror symmetry in the generated beam. In addition, we have shown that the beam maintains its morphology even if con/diverging (as in terms of focusing).

2. Methodology

The main idea of this work was to create a beam shape with a temporally changing intensity pattern. One possibility is to generate two different frequency beams separately and to make them interfere by conventional optical means, such as combining imaging optics and beam splitters or by using a holographic liquid crystal on a silicon spatial light modulator or SLM; however, such an element is very slow. Our method allows us to achieve a spiralling interference intensity pattern by causing interference of chirped and slightly shifted beams with a different topological charge. As the optical frequency of light is in the petahertz range, the slight shift would have a beating that is still very fast and would allow dynamic shape changes in the picosecond timeframe. By delaying one of the chirped pulses in relation to the other, they would interfere with a slightly shifted optical frequency [28]. The frequency shift will change the corresponding rotation speed $\delta\omega = \omega(t) - \omega(t - \delta t)$. If these chirped pulses have an orbital angular momentum and propagate as intensity rings, their interference will result in an intensity pattern comprised of the maxima based on the orbital angular momentum (OAM) difference $\Delta l = l_2 - l_1$. The final resultant beam will be a tube with multiple maxima rotating in time. If we would assemble the time frames of a single spatial zone, we would get a spiralling intensity pattern rotating at THz frequency.

The interfering beams have a spatial amplitude distribution given by the function

$$E = \frac{E_0}{\omega}\left(\frac{r}{\omega}\right)^l \exp\left(-\frac{r^2}{\omega^2} - \mathrm{i}\varphi l\right), \quad (1)$$

where l is the topological charge or OAM, and ω is the beams waist. The chirped Gaussian pulse temporal amplitude distribution has the form:

$$E_{1p} = \exp\left[-\frac{t^2}{\tau_{\mathrm{chirp}}}(1 + \mathrm{i}\gamma)\right], \quad (2)$$

$$E_{2p} = \exp\left[-\frac{(t + T_{\mathrm{shift}})^2}{\tau_{\mathrm{chirp}}}(1 + \mathrm{i}\gamma)\right]. \quad (3)$$

Here τ_{chirp} is the chirped pulse duration, T_{shift} is the time delay between pulses, and γ is the chirp parameter defined as

$$\gamma = \sqrt{(\tau_{\mathrm{chirp}} / \tau_0)^2 - 1}, \quad (4)$$

where τ_0 is the transform limited pulse duration. The interference of two beams is expressed as a superposition

$$E_{\mathrm{tot}} = E_{\mathrm{LG1}}E_{1p} + E_{\mathrm{LG2}}E_{2p}. \quad (5)$$

The spatiotemporal intensity distribution of the beam can be found by $I_{\mathrm{tot}} = |E_{\mathrm{tot}}|^2$. The resultant helical beam will twist in time, as shown in Fig. 1. The rotation speed will be determined by two parameters: (i) the chirp induced to both pulses and (ii) the delay time between the chirped pulses. For a given chirp of both pulses, the induced rotation will increase linearly with an increase in the delay, whereas pulses with the same delay but a smaller chirp will rotate faster.

3. Experimental setup

To experimentally demonstrate the generation of rotating maxima intensity beams, a setup based on q-plates can form a light beam with an orbital angular momentum from a beam with a spin angular

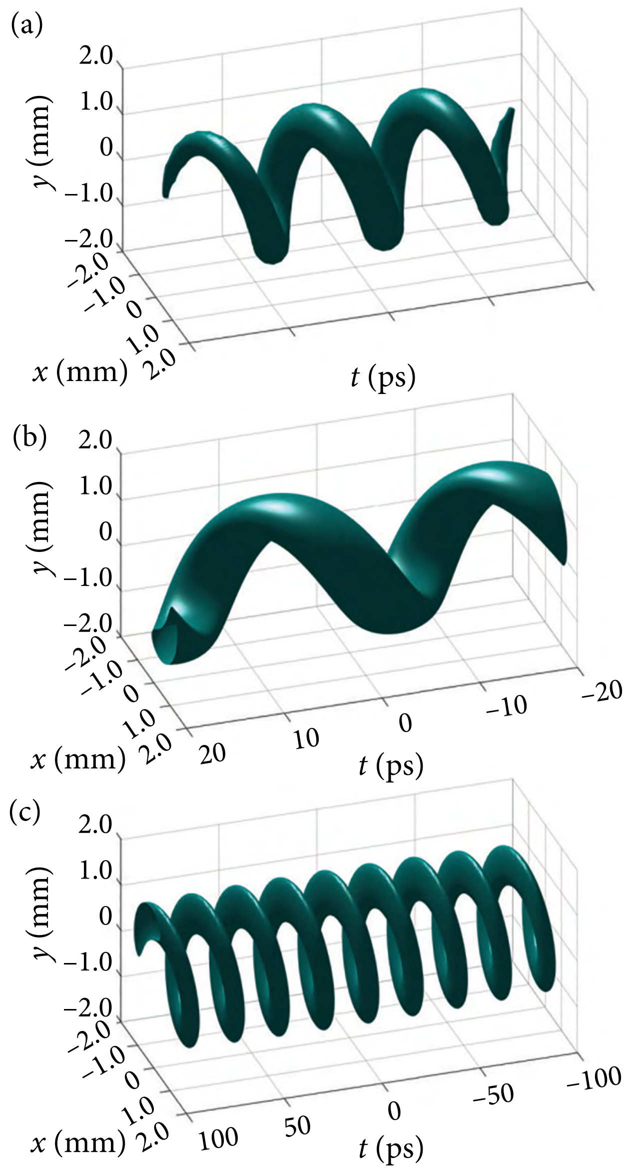

Fig. 1. Numerically simulated 3D isosurfaces of the helical beams. (a) Helical beam with a shift of 2 ps and a chirped pulse duration of 50 ps. (b) shows a helical beam with a shift of 2 ps and a chirped pulse duration of 500 ps, while (c) has a delay time of 10 ps and a chirped pulse duration of 500 ps. The transform limited pulse duration was set to 200 fs in all cases.

momentum (circular polarization). Also, the two beams must be mutually coherent to give a steady rotation of the interference pattern. The mixing from the two separate lasers would give random jumps to the intensity pattern on top of the dominating rotation, with the average time between the jumps equal to the mutual coherence time. Our solution was to use a single laser light source and split it with beam splitters. In this work, we used a Yb:KGW femtosecond laser 'Carbide' (*UAB Light Conversion*), providing radiation at the 1030 nm fundamental wavelength, the 200 fs pulse duration and the 250 kHz repetition rate. The initial laser beam was split in two with a non-polarizing beamsplitter. One part was sent to a delay line, was maintained at 200 fs and was used for gating the other beam, while the rest of the beam went to the stretcher made from two diffraction gratings and a retro reflector. This stretcher was used to form the chirped beams needed to create the helical intensity. Their generated interference pattern would then rotate proportionally to the mismatch of the path lengths of each chirped pulse. The laser beam is then passed through a $\lambda/2$ phase plate and a polarizing beamsplitter to equalize the powers of each of the beams and has a linear polarization. Polarizations of each beam were changed to circular ones and a different topological charge was imparted onto the beams by a polarization-sensitive spiral phase plate similar to that in Ref. [21]. When this circularly polarized beam passes through the q-plate, it becomes a circularly polarized vortex beam, which is converted back to a linear polarization without changing the vortex phase by a polarizing plate. One of the chirped beams was sent to another delay line to tune the arrival time, and this enabled a variable delay between the chirped pulses. And finally, the beams were joined together by another non-polarizing beamsplitter. A polarizing plate was used to select only a linear polarization for the second harmonic generation of the second type. A final mirror was used to send the co-axial beams to a BBO second harmonic crystal. A WinCamD DataRay CCD with a 4.4 μm pixel size was used for capturing the intensity patterns. The schematic of this system is given in Fig. 2.

4. Results and discussion

Because the structure is not clearly visible due to the fast rotation, to detect and reconstruct the pattern a second harmonic cross-correlator was used to 'freeze' the structure in time and probe its true shape and parameters. By using the second type of the second harmonic generation (eo-e) we will only generate it by beams of different polarization. The interfering LG beams were of one polarization and the short Gauss pulse was of the opposite linear polarization. Intersecting at an angle they generated

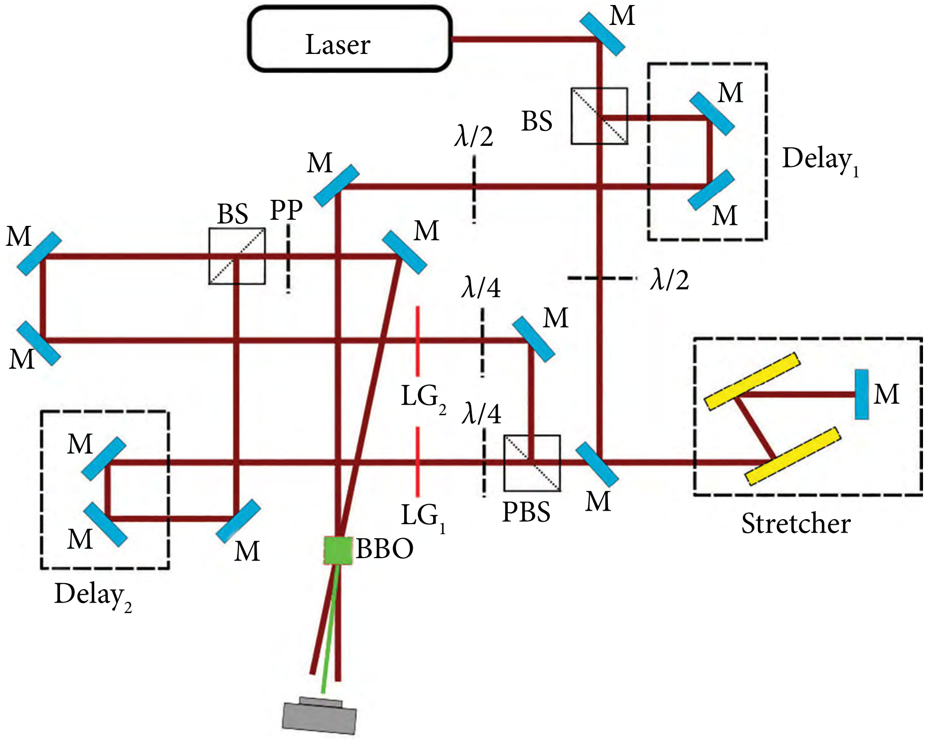

Fig. 2. Optical scheme used for beam interference and gating. $\lambda/2$ waveplates are used to perpendicularly align the polarization states of the interfering beams and Gauss beams. $\lambda/4$ waveplates are used to create a circular polarization for LG generation. $Delay_1$ and $Delay_2$ are delay lines to tune the arrival time of both the Gauss gate and the delay of the chirped beams, LG are Laguerre–Gauss mode q-plates, M are mirrors, PBS are polarizing beamsplitters, BS are non-polarizing beamsplitters, and PP is a polarizing plate. A BBO crystal is used for the second harmonic (2H) generation. The intensity distribution was measured on the CCD camera of the spatially modulated beam. A beam stretcher was used to chirp part of the initial short pulse.

the second harmonic with a 'frozen' intensity pattern as seen in Fig. 3. We had the ability to place a lens before the BBO crystal to focus the beam.

We showed the initial second harmonic generation result without focusing. This allowed us to tune the parameters of the resultant helical structure more easily. By using a variety of spiral phase plates with topological charges (l = 1, 2, 3) different variations of chirped rotating beams were probed, as can be seen in Fig. 3. The total number of maxima matches the topological charge difference between the interfering beams. By changing the handedness of the circular polarization, the sign of the topological charge can be inverted, allowing the creation of even more pairs. Pulse powers were kept similar for better interference results. Small intensity fluctuations and deviations are from not ideally collinear beams. The number of

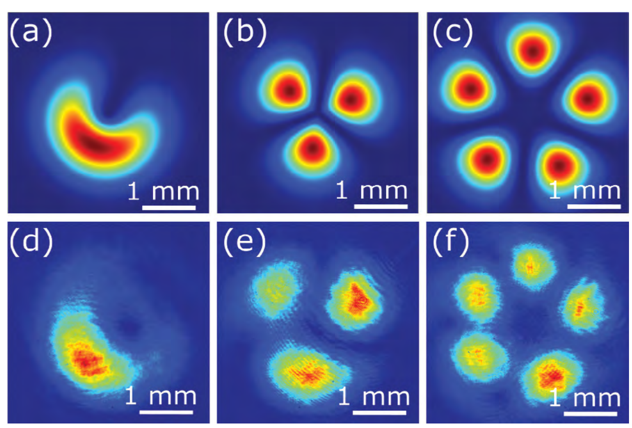

Fig. 3. *xy* cross-section comparison. (a–c) are numerically simulated intensity patterns of 2H generation between a Gaussian pulse and two interfering chirped beams, while (d–f) are the corresponding experimental measurements. The corresponding topological charge pairs are the following: 1 and 2; 1 and –2, –2 and 3.

maxima can be easily tuned by changing the plates in the scheme. Also, by changing the handedness of the circularly polarized light, the topological charges can be flipped.

Experimental *xy* cross sections of the first harmonic of the beam in Fig. 4(a–c) show that the *true* intensity shape quickly disappears if the delay between the chirped pulses is more than 5 ps (Fig. 4(a)). A focusing lens of 100 mm focal length was used to see how the structure scales and whether it loses its shape. As seen in Fig. 4(d–f), even the defects present in the large structure are maintained in the focal region.

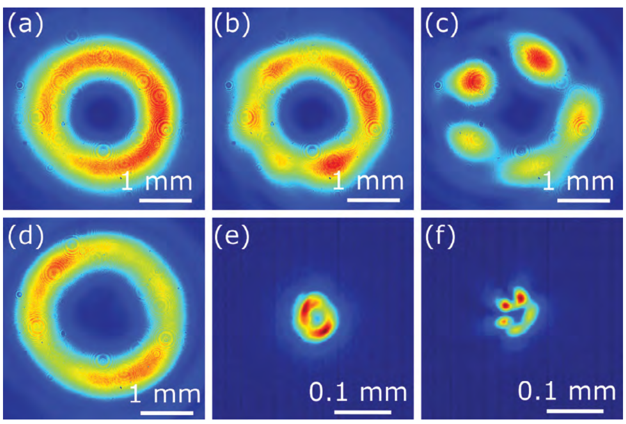

Fig. 4. Experimental observation of *xy* cross-section intensity patterns. (a–c) Intensity pattern of the 1H interference pattern with a delay between pulses of 5.4, 2.7 and 0 ps, respectively. (d) Intensity pattern of one of the chirped pulses with a topological charge of 3. (e) Intensity pattern of a chirped pulse with topological charge 3 focused by a 100 mm focal lens. (f) Interference pattern with no delay between pulses focused by 100 mm focal lens.

For micromachining applications, we must note that the induced chirp decreases the intensity of the laser beam. However, the chirp does not need to be drastic. The large chirp value used in the experiment was for visualization purposes. We have used the probe pulse of 200 fs duration, therefore the rotation period had to be much longer than that. We think that such a beam can be easily implemented into a direct laser writing system for microfabrication or other usages. The most complicated part is assuring the coaxial propagation of both beamlines which can be done with a careful alignment. The structure is highly tuneable: by varying the delay of one line, the rotation speed can be tuned and even its rotation direction can be flipped. Alternatively, by using higher topological charges, different numbers of high-intensity zones can be formed. This beam maintains its shape when focused; therefore, implementation into a more practical system is feasible. The drill is expected to interact with the material primarily through thermal effects, phonon excitations, and relaxations. The fast rotation in THz ranges can possibly result in interesting interaction effects; however, a detailed analysis of wave–matter interaction is out of the scope of the article.

5. Conclusions

In this work, we applied a practical method for generating fast-rotating vortex–pulse pair beams by causing interference of two higher-order Laguerre–Gauss beams. Although the principles have been demonstrated before, we confirm their reproducibility using *odd* Δl values, which do not feature mirror symmetry.

To probe the fast-rotating spatial structure, a shorter Gauss pulse was used for the second harmonic generation in a cross-correlator setup. The time-varying 3D structure was numerically simulated, and the 2D cross-sections were measured and even reimaged. Like the stationary optical drill beams, the vortex–pulse pair could become useful for particle micromanipulation and micromachining. This article confirms the main principle and experimental observations and provides confidence for further studies that deal with the light–matter interaction using pulses with higher energy and intensities.

Acknowledgements

The authors are grateful to dr. Domas Paipulas from Vilnius University for lending the experimental equipment, dr. Simas Butkus for helping to set up the pulse stretcher, and *Workshop of Photonics* (Ltd.) for supplying the q-plates used in the experiment.

The authors D. Gailevičius and G. Kontenis acknowledge funding from the Research Council of Lithuania (Grant No. S-MIP-23-49).

References

[1] G. Kamlage, T. Bauer, A. Ostendorf, and B.N. Chichkov, Deep drilling of metals by

femtosecond laser pulses, Appl. Phys. A **77**, 307–310 (2003), https://doi.org/10.1007/s00339-003-2120-x

[2] K.H. Leitz, B. Redlingshöer, Y. Reg, A. Otto, and M. Schmidt, Metal ablation with short and ultrashort laser pulses, Phys. Procedia **12**, 230–238 (2011), https://doi.org/10.1016/j.phpro.2011.03.128

[3] K. Sugioka and Y. Cheng, Ultrafast lasers-reliable tools for advanced materials processing, Light Sci. Appl. **3**, 1–12 (2014), https://doi.org/10.1038/lsa.2014.30

[4] D. Nieto, J. Arines, G.M. O'Connor, and M.T. Flores-Arias, Single-pulse laser ablation threshold of borosilicate, fused silica, sapphire, and soda-lime glass for pulse widths of 500 fs, 10 ps, 20 ns, Appl. Opt. **54**, 8596 (2015), https://doi.org/10.1364/ao.54.008596

[5] B.N. Chichkov, C. Momma, S. Nolte, F. Von Alvensleben, and A. Tünnermann, Femtosecond, picosecond and nanosecond laser ablation of solids, Appl. Phys. A **63**, 109–115 (1996), https://doi.org/10.1007/BF01567637

[6] S. Butkus, V. Jukna, D. Paipulas, M. Barkauskas, and V. Sirutkaitis, Micromachining of invar foils with GHz, MHz and kHz femtosecond burst modes, Micromachines **11**, 733 (2020), https://doi.org/10.3390/MI11080733

[7] Y. Horie, A. Arbabi, E. Arbabi, S.M. Kamali, and A. Faraon, High-speed, phase-dominant spatial light modulation with silicon-based active resonant antennas, ACS Photonics **5**, 1711–1717 (2018), https://doi.org/10.1021/acsphotonics.7b01073

[8] R. Ivaškevičiūtė-Povilauskienė, P. Kizevičius, E. Nacius, D. Jokubauskis, K. Ikamas, A. Lisauskas, N. Alexeeva, I. Matulaitienė, V. Jukna, S. Orlov, L. Minkevičius, and G. Valušis, Terahertz structured light: nonparaxial Airy imaging using silicon diffractive optics, Light Sci. Appl. **11**, 326 (2022), https://doi.org/10.1038/s41377-022-01007-z

[9] D. Flamm, D.G. Grossmann, M. Sailer, M. Kaiser, F. Zimmermann, K. Chen, M. Jenne, J. Kleiner, J. Hellstern, C. Tillkorn, D.H. Sutter, and M. Kumkar, Structured light for ultrafast laser micro- and nanoprocessing, Opt. Eng. **60**, 025105 (2021), https://doi.org/10.1117/1.oe.60.2.025105

[10] S.D. Gittard, A. Nguyen, K. Obata, A. Koroleva, R.J. Narayan, and B.N. Chichkov, Fabrication of microscale medical devices by two-photon polymerization with multiple foci via a spatial light modulator, Biomed. Opt. Express **2**, 3167 (2011), https://doi.org/10.1364/boe.2.003167

[11] E. Stankevicius, T. Gertus, M. Rutkauskas, M. Gedvilas, G. Raciukaitis, R. Gadonas, V. Smilgevicius, and M. Malinauskas, Fabrication of micro-tube arrays in photopolymer SZ2080 by using three different methods of a direct laser polymerization technique, J. Micromech. Microeng. **22**, 065022 (2012), https://doi.org/10.1088/0960-1317/22/6/065022

[12] L. Zhao, L. Huang, J. Huang, K. Xu, M. Wang, S. Xu, and X. Wang, Far-field parallel direct writing of sub-diffraction-limit metallic nanowires by spatially modulated femtosecond vector beam, Adv. Mater. Technol. **7**, 2200125 (2022), https://doi.org/10.1002/admt.202200125

[13] R.D. Simmonds, P.S. Salter, A. Jesacher, and M.J. Booth, Three dimensional laser microfabrication in diamond using a dual adaptive optics system, Opt. Express **19**, 24122 (2011), https://doi.org/10.1364/oe.19.024122

[14] B.P. Cumming, A. Jesacher, M.J. Booth, T. Wilson, and M. Gu, Adaptive aberration compensation for three-dimensional micro-fabrication of photonic crystals in lithium niobate, Opt. Express **19**, 9419 (2011), https://doi.org/10.1364/oe.19.009419

[15] P.S. Salter, M. Baum, I. Alexeev, M. Schmidt, and M.J. Booth, Exploring the depth range for three-dimensional laser machining with aberration correction, Opt. Express **22**, 17644 (2014), https://doi.org/10.1364/oe.22.017644

[16] A. Jesacher and M.J. Booth, Parallel direct laser writing in three dimensions with spatially dependent aberration correction, Opt. Express **18**, 21090 (2010), https://doi.org/10.1364/oe.18.021090

[17] B. Wetzel, C. Xie, P.A. Lacourt, J.M. Dudley, and F. Courvoisier, Femtosecond laser fabrication of micro and nano-disks in single layer graphene

using vortex Bessel beams, Appl. Phys. Lett. **103**, 24111 (2013), https://doi.org/10.1063/1.4846415

[18] R. Bowman, N. Muller, X. Zambrana-Puyalto, O. Jedrkiewicz, P. Di Trapani, and M.J. Padgett, Efficient generation of Bessel beam arrays by means of an SLM, Eur. Phys. J. Spec. Top. **199**, 159–166 (2011), https://doi.org/10.1140/epjst/e2011-01511-3

[19] N. Bozinovic, Y. Yue, Y. Ren, M. Tur, P. Kristensen, H. Huang, A.E. Willner, and S. Ramachandran, Terabit-scale orbital angular momentum mode division multiplexing in fibers, Science **340**, 1545–1548 (2013), https://science.sciencemag.org/content/sci/340/6140/1545.full.pdf

[20] M. Martyanov, V. Ginzburg, A. Balakin, S. Skobelev, D. Silin, A. Kochetkov, I. Yakovlev, A. Kuzmin, S. Mironov, I. Shaikin, S. Stukachev, A. Shaykin, E. Khazanov, and A. Litvak, Suppressing small-scale self-focusing of high-power femtosecond pulses, High Power Laser Sci. Eng. **11**, e28 (2023), https://doi.org/10.1017/hpl.2023.20

[21] Z. Chen, S. Zheng, X. Lu, X. Wang, Y. Cai, C. Wang, M. Zheng, Y. Ai, Y. Leng, S. Xu, and D. Fan, Forty-five terawatt vortex ultrashort laser pulses from a chirped-pulse amplification system, High Power Laser Sci. Eng. **10**, 1–7 (2022), https://doi.org/10.1017/hpl.2022.19

[22] S. Jiménez-Gambín, N. Jiménez, J.M. Benllo, F. Camarena, J.M. Benlloch, and F. Camarena, Generating Bessel beams with broad depth-of-field by using phase-only acoustic holograms, Sci. Rep. **9**, 1–13 (2019), https://doi.org/10.1038/s41598-019-56369-z

[23] G. Kontenis, D. Gailevičius, N. Jiménez, and K. Staliunas, Optical drills by dynamic high-order Bessel beam mixing, Phys. Rev. Appl. **17**, 1–7 (2022), https://doi.org/10.1103/physrevapplied.17.034059

[24] N.J. González, K. Staliunas, and F. Camarena, *Sistema y método de generación de haces acústicos confocales de vórtice con superposición espacio temporal*, Spanish Patent P202030766 (2020), European Patent ES2811650 (2021), G01N29/22,A61N 7/00,B06B 1/06.

[25] N. Jiménez, V. Romero-García, R. Picó, A. Cebrecos, V.J. Sánchez-Morcillo, L.M. Garcia-Raffi, J.V. Sánchez-Pérez, and K. Staliunas, Acoustic Bessel-like beam formation by an axisymmetric grating, Europhys. Lett. **106**, 24005 (2014), https://doi.org/10.1209/0295-5075/106/24005

[26] N. Jiménez, R. Picó, V. Sánchez-Morcillo, V. Romero-García, L.M. García-Raffi, and K. Staliunas, Formation of high-order acoustic Bessel beams by spiral diffraction gratings, Phys. Rev. E. **94**, 053004 (2016), https://doi.org/10.1103/PhysRevE.94.053004

[27] S. Franke-Arnold, J. Leach, M.J. Padgett, V.E. Lembessis, D. Ellinas, A.J. Wright, J.M. Girkin, P. Öhberg, and A.S. Arnold, Optical ferris wheel for ultracold atoms, Opt. InfoBase Conf. Pap. **15**, 169–175 (2007), https://doi.org/10.1364/cqo.2007.cmi3

[28] K. Yamane, M. Sakamoto, N. Murakami, R. Morita, and K. Oka, Picosecond rotation of a ring-shaped optical lattice by using a chirped vortex-pulse pair, Opt. Lett. **41**, 4597 (2016), https://doi.org/10.1364/ol.41.004597

[29] A. Honda, K. Yamane, K. Iwasa, K. Oka, Y. Toda, and R. Morita, Ultrafast beam pattern modulation by superposition of chirped optical vortex pulses, Sci. Rep. **12**, 1–12 (2022), https://doi.org/10.1038/s41598-022-18145-4

ČIRPUOTŲ LAGERO IR GAUSO MODŲ INTERFERENCIJOS SUFORMUOTI CHIRALINIAI PLUOŠTAI

G. Kontenis [a], **D. Gailevičius** [a], **V. Jukna** [a], **K. Staliūnas** [a, b, c]

[a] *Vilniaus universiteto Lazerinių tyrimų centras, Vilnius, Lietuva*

[b] *Katalonijos politechnikos universiteto Fizikos ir branduolinės inžinerijos katedra, Terasa, Ispanija*

[c] *Katalonų tyrimų ir aukštųjų studijų institutas (ICREA), Barselona, Ispanija*

Santrauka

Šiame darbe tiriama greitai laike besisukančio interferencinio pluošto struktūra ir jo erdviniai parametrai. Tokio tipo struktūros yra realizuojamos suvedant du koherentinius pluoštus su topologiniu krūviu / orbitiniu judesio kiekio momentu. Jeigu jų topologiniai krūviai skiriasi, gaunamas pluoštas su maksimumų skaičiumi, lygiu abiejų pluoštų topologinių krūvių skirtumui. Toks pluoštas laike yra statiškas, norint indukuoti jam sukimąsi reikia laike moduliuoti vieno iš pluoštų fazę. Tai galima atlikti elektrooptiniais ar akustooptiniais moduliatoriais, tačiau tokie sprendimai lemia sąlyginai lėtą sukimąsi. Šiame darbe pademonstruotas laike moduliuoto spiralinio intensyvumo pasiskirstymo pluošto, kurio sukimąsi laike galima keisti, formavimo metodas. Tai įgyvendinama interferuojant du kolinearius čirpuotus ir laike pastumtus impulsus. Pateikiami analitiniai ir skaitiniai rezultatai bei parodomas eksperimentinis tokios struktūros realizavimas. Skirtingai nuo ankstesnių darbų [28, 29], čia parodoma realizacija nelyginių topologinių krūvių atvejais, kai nėra simetrijos apie nulį. Tikėtina, kad pluoštas su laikine moduliacija pikosekundinėje skalėje turės teigiamo poveikio šiluminiam režimui šviesai sąveikaujant su medžiaga.